Structural Safety xxx (2010) xxx–xxx

Contents lists available at ScienceDirect

Structural Safety

journal homepage: www.elsevier.com/locate/strusafe

Computational intelligence methods for the efficient reliability analysis of complex flood defence structures

Greer B. Kingston [a], Mohammadreza Rajabalinejad [b], Ben P. Gouldby [a,*], Pieter H.A.J.M. Van Gelder [b]

[a] HR Wallingford Ltd., Howbery Park, Wallingford, Oxfordshire OX10 8BA, United Kingdom
[b] Faculty of Civil Engineering and Geosciences, Delft University of Technology, 2600 GA Delft, The Netherlands

ARTICLE INFO

Article history:
Received 24 November 2008
Received in revised form 12 August 2010
Accepted 19 August 2010
Available online xxxx

Keywords:
Flood defence
Structural reliability
Artificial neural networks
Genetic algorithms
Adaptive sampling
Response surface function

ABSTRACT

With the continual rise of sea levels and deterioration of flood defence structures over time, it is no longer appropriate to define a design level of flood protection, but rather, it is necessary to estimate the reliability of flood defences under varying and uncertain conditions. For complex geotechnical failure mechanisms, it is often necessary to employ computationally expensive finite element methods to analyse defence and soil behaviours; however, methods available for structural reliability analysis are generally not suitable for direct application to such models where the limit state function is only defined implicitly. In this study, an artificial neural network is used as a response surface function to efficiently emulate the complex finite element model within a Monte Carlo simulation. To ensure the successful and robust implementation of this approach, a genetic algorithm adaptive sampling method is designed and applied to focus sampling of the implicit limit state function towards the limit state region in which the accuracy of the estimated response is of the greatest importance to the estimated structural reliability. The accuracy and gains in computational efficiency obtainable using the proposed method are demonstrated when applied to the 17th Street Canal flood wall which catastrophically failed when Hurricane Katrina hit New Orleans in 2005.

1. Introduction

Floods are a widespread and potentially devastating natural hazard. Recent serious flood events throughout the world, such as the 2002 and 2005 European floods, the New Orleans event in 2005 [1,2] and the 2007 UK summer floods [3], have prompted a shift away from flood protection policies that consider a 'standard of protection' towards risk-based flood assessment methods, which take into account the probability of flooding and the related consequences. In much of the developed world, the probability of flooding has been modified by the construction of flood defences (e.g. dikes, flood gates), which form an important part of a broader approach to integrated flood risk management. Thus, to support credible estimates of the probability of flood inundation, the structural reliability of flood defences, given uncertain strength and loading conditions, must be taken into account.

In traditional structural reliability analysis, failure of a structure arises when the loads acting upon the structure, S, exceed its bearing capacity, or resistance, R. Here, R and S are functions of the basic random variables $\mathbf{X} = \{X_i,\ i = 1,\ldots,K\}$, which describe the material properties of, and the external loads applied to, the structure. The problem is then typically presented in the following generalised form [4]:

$$P_f = P[g(R,S) \leqslant 0] = \int_{g(R,S)\leqslant 0} f_{\mathbf{X}}(\mathbf{x})d\mathbf{x} \tag{1}$$

where P_f gives the probability of failure; $f_{\mathbf{X}}(\mathbf{x})$ is the multivariate probability density function of $\mathbf{X}$; and $g(R,S)$ is the well known limit state function (LSF), which is often defined as $g(\mathbf{X}) = R - S$. In system based flood risk analysis models, where series of flood defences protect urban areas and there is a requirement to model the consequences of failure in terms of damage to infrastructure through inundation, it can be convenient to consider the *fragility* of individual flood defence cross-sections (e.g. see [5]), which is the probability of failure conditional on loading, defined by:

$$P_f = P[g(\mathbf{X}) \leqslant 0 | S = s] \tag{2}$$

In some cases, the relationships between R and S are known explicitly and $g(\mathbf{X})$ can be expressed in closed form (or the problem can be suitably simplified such that this is the case). However, in other more complex cases, such as those involving geotechnical instabilities, the LSF can only be evaluated implicitly through a more complex numerical model, such as a finite element (FE) model. For the majority of flood defences, a simplified numerical method (e.g.

* Corresponding author.
E-mail addresses: g.kingston@hrwallingford.co.uk (G.B. Kingston), b.gouldby@hrwallingford.co.uk (B.P. Gouldby).

0167-4730/$ - see front matter © 2010 Published by Elsevier Ltd.
doi:10.1016/j.strusafe.2010.08.002

Bishop's simplified method) may suffice and, in many cases, will be all that the limited available geotechnical data lends itself to. However, for more critical defences whose failure would result in catastrophic flooding (e.g. storm surge barriers; defences that protect areas lying below sea level in the Netherlands and New Orleans), a full finite element (FE) analysis may be warranted. In these cases, evaluating the probability of failure of the flood defence can be problematic for reasons discussed as follows.

For all but the simplest cases, the integral in (1) is analytically intractable and some method is required to estimate *Pf*. Methods available for this include gradient-based methods (the so-called FORM and SORM approaches) and simulation-based methods (e.g. Monte Carlo methods, Riemann integration) [4]. However, neither of these approaches is directly suitable for estimating the probability of complex flood defence failures where evaluation of the LSF is implicit. The former methods require explicit knowledge of the LSF, as it is necessary to estimate the gradient of the LSF with respect to the basic variables, whilst the latter, simulation-based approaches can be computationally prohibitive, since, for each realisation of the basic random variables, a complete FE analysis is required, which itself requires considerable computational effort.

To overcome the difficulties associated with complex reliability analyses, a number of authors have proposed the use of the Response Surface Method (RSM) [6–9], whereby a so-called response surface function (RSF), which is a more computationally efficient and explicit mapping of the response surface, is used as a *surrogate* or *emulator* of the actual response surface. In the original RSM, RSFs commonly take the form of low order polynomials (usually quadratic). However, the accuracy of such functions in approximating the shape of the actual LSF is limited due to the rigid and non-adaptive structure assumed [10]. This, in turn, limits the accuracy of the estimated P_f. More recently, artificial neural networks (ANNs) have been proposed as alternative RSFs to those employed using the RSM [10–17]. These models have been shown to outperform the traditional RSM due to their superior mapping capabilities and flexible functional form [10]. ANNs also have the advantage of being applicable to higher dimensional problems than the traditional RSM [18].

Despite these advantages, ANNs have not been widely used in reliability analyses of complex systems due to the large number of implicit LSF evaluations that are still required for fitting the ANN model. In most applications of ANN-based RSFs, samples have been generated by standard Monte Carlo simulation (MCS), which may lead to an insufficient covering of the mapping domain, particularly for problems with low failure probability. This is illustrated in Fig. 1, which shows that, using standard MCS, the most probable sampling domain results in limited samples about the limit state $g(\mathbf{X}) = 0$, even if the number of samples is large. This would then lead to an inadequate description of the limit state, which is the region of the actual response surface that must be represented most accurately for the successful application of RSFs in reliability analyses. However, attempts to reduce any inaccuracies in the limit state description by generating a larger set of samples for fitting the ANN then leads to a required effort comparable to direct MCS with the complex FE model.

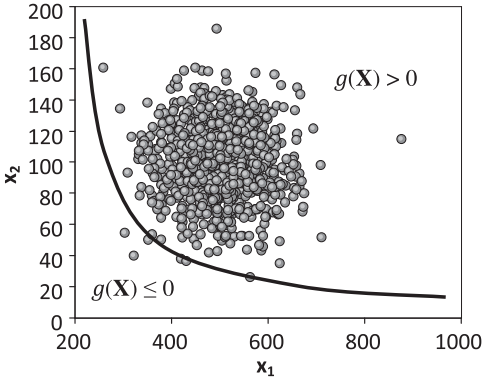

Fig. 1. Inadequate coverage of the mapping domain obtained with standard MCS.

Whilst a variety of importance sampling strategies have been proposed, these are not without their limitations [4]. In this paper, a new adaptive sampling technique based on a genetic algorithm (GA) is presented for focusing the sampling of the actual LSF towards the limit state. This method exploits the population-based search and exploration capabilities of GAs to provide efficient coverage of the entire parameter space with the most densely sampled area being that around the limit state $g(\mathbf{X}) = 0$. This enables the most accurate mapping of the ANN-based RSF in the most important region.

The remainder of this paper is structured as follows: in Section 2, the development of an ANN-based RSF for flood defence reliability analysis is described, whilst in Section 3, the new GA adaptive sampling method used to help train the ANN is presented, together with its advantages over conventional sampling regimes. In Section 4, application of the ANN together with the GA adaptive sampling approach is demonstrated in a case study involving the reliability analysis of the 17th Street flood wall, which catastrophically failed when Hurricane Katrina hit New Orleans. The use of the ANN-based RSF in a Monte Carlo based reliability analysis is compared to direct MCS of the actual implicit LSF in order to assess the accuracy and efficiency of the proposed method and the results are discussed in relation to their implications for flood risk modelling and management. Finally, in Section 5, the conclusions of the paper are drawn.

2. ANN-based RSF

Whilst the LSF describing a complex failure mechanism may not be known explicitly, for N limited discrete samples of $\mathbf{X} = \mathbf{x}_n$, where $n = 1,\ldots,N$, the implicit LSF $g(\mathbf{x}_n)$ can be evaluated. The aim in developing a RSF is to find the explicit function $\bar{g}(\mathbf{X})$ that provides the best fit to the set of discrete samples $\{g(\mathbf{x}_n),\ n = 1,\ldots,N\}$. It is then assumed that if the approximating function $\bar{g}(\mathbf{X})$ fits the discrete samples sufficiently well, particularly in the region around the actual limit state $g(\mathbf{X}) = 0$, a reliable estimate of the probability of failure can be obtained. However, one of the difficulties associated with this approach lies in the fact that the limit state in most realistic structural problems has a highly nonlinear, yet unknown, functional form [9] and that this function is difficult to approximate to a sufficient degree of accuracy given only limited discrete samples of $\mathbf{X}$.

ANNs are especially suited for use as RSFs, as they are able to extract a complex, nonlinear input–output mapping from synthetic data samples without in-depth knowledge of the underlying implicit LSF. Furthermore, once developed, ANNs are relatively quick to run; the necessary characteristic that makes RSFs valuable in situations where quick estimation is required (e.g. in MCS where repeated evaluations of the LSF are performed). A significant advantage of the ANN modelling approach over the more traditional polynomial RSFs is that, being data-driven and model-free, ANNs do not require any restrictive assumptions about the functional form of the LSF, as the latter methods do. In fact, their flexible functional form makes it possible for ANNs to model any continuous function to an arbitrary degree of accuracy and, as such, they are often considered to be 'universal function approximators' [19,20].

Originally designed to mimic the functioning of the brain [21], ANNs are composed of a number of highly interconnected processing units called nodes or *neurons*. Individually, these nodes only

Please cite this article in press as: Kingston GB et al. Computational intelligence methods for the efficient reliability analysis of complex flood defence structures. Struct Saf (2010), doi:10.1016/j.strusafe.2010.08.002

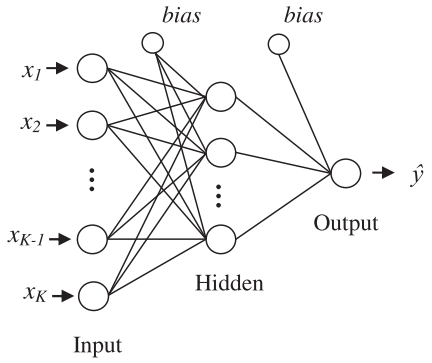

Fig. 2. Layer structure of a MLP.

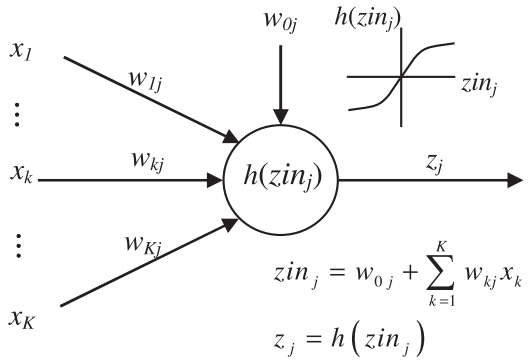

Fig. 3. Operation of a single node.

carry out rather simple and limited computations; however, collectively as a network, complicated computations can be performed due to the connectivity between the nodes and the way in which information is passed through and processed within the network. Multilayer perceptrons (MLPs), which are a popular and widely used type of ANN, were used in this study. As their name suggests, these ANNs are made up of several layers of nodes. The nodes are arranged into an input layer, an output layer and one or more intermediate layers, called 'hidden' layers, as shown in Fig. 2. A general description of a MLP and its mathematics is given in Appendix A.

When an ANN is used to approximate the LSF, each sample of the basic variables $\mathbf{x}_n = \{x_{i,n},\ i = 1,\ldots,K\}$ is received at the input layer, which contains K nodes corresponding to the K basic stress and resistance variables. This information is then transmitted to each node in the next layer via weighted connections, where the weight determines the strength of the incoming signal. At the nodes, the weighted information is summed together with a bias value and transferred using pre-defined (usually) nonlinear activation functions, before being transmitted to the nodes in subsequent layers. This process is shown in Fig. 3. The signal $\hat{y}$ generated at the output layer is the predicted value related to $\bar{g}(\mathbf{x})$. ANN-based RSFs can either be used for functional approximation, where $\hat{y}_n = \bar{g}(\mathbf{x}_n)$, or for data classification, where $\hat{y}_n = I[\bar{g}(\mathbf{x}_n) \leqslant 0]$ and where $I[\cdot]$ is an indicator function equal to 0 or 1 dependent on whether the sample $\mathbf{x}_n$ is in the failure or safe domain.

In order for the network to perform the desired function, appropriate values of the network weights, $\mathbf{w}$, which are the free parameters of the model, must be estimated. This is carried out through a process known as *training* (calibration), where the model outputs y are compared to the target values $y = g(\mathbf{x})$ or $y = I[g(\mathbf{x}) \leqslant 0]$ and the weights are iteratively adjusted to minimise the difference, or error, between these values. The appropriate complexity of the ANN must also be selected, where complexity is adjusted by increasing or decreasing the number of hidden nodes. In general applications of ANNs, it is often desirable to minimise the complexity such that the model does not overfit to noise in the training data. However, there will not be any noise in synthetic data generated from a simulation model and, therefore, overfitting is not a concern. Nevertheless, in the interests of parsimony, efforts should be made to select the smallest network able to adequately capture the underlying relationship in the data.

3. Genetic algorithm adaptive sampling

The success of an ANN-based RSF hinges on the quality of the training data used for developing the model. This data set must represent the overall domain in which values of $\mathbf{X}$ are likely to be obtained by simulation. In [17,22], it was argued that, in order to avoid the situation illustrated in Fig. 1 and to achieve a valid ANN-based RSF, the training data should be selected as uniformly as possible across the variable space. However, when there is a practical computational constraint on the number of training samples that can be taken, it is much more important that the region about the limit state $g(\mathbf{X}) = 0$ is accurately represented, as the estimated Pf is most sensitive to discrepancies between $\bar{g}(\mathbf{X})$ and $g(\mathbf{X})$ in this is the region, as illustrated in Fig. 4. Therefore, a more accurate ANN approximation of the actual LSF can be obtained if sampling is focused towards the region about the limit state and fewer samples are taken elsewhere.

GAs are a general purpose stochastic search technique that can be used to solve complex optimisation problems. In the application presented in this paper, a GA is used to optimise the sampling process used to obtain a suitable training set for fitting the ANN-based RSF. This method is based upon that employed by Khu and Werner [23], where a GA was also used for mapping the response surface of a computationally intensive model.

Inspired by Darwin's theory of natural selection and survival of the fittest, GAs work by employing genetics-inspired operators such as *selection, crossover* and *mutation* to evolve from one *population* of solutions to the next by selectively sharing information among the 'fittest' members. The evolutionary process starts from a completely random population and occurs over a number of successive iterations, or *generations*, where the new population formed in one generation becomes the population from which a new population is evolved in the next, and so forth.

If the problem is defined such that samples lying on the limit state are assigned the maximum fitness level, the GA adaptive sampling process can be set up such that it begins by sampling uniformly across the entire feasible variable space, but, over a number of generations, focuses sampling towards the region about the limit state surface. Typically, when a GA is used for optimisation, initial generations are discarded and only the final fittest member, or set of members, are retained. However, it is the initial generations of the adaptive sampling process that provide the overall, albeit coarse, representation of the entire domain of $\mathbf{X}$. Therefore, using this method, all samples are retained from the first generation to the last, to enable a coarse uniform coverage of the entire domain of $\mathbf{X}$, with significantly more detail provided in the important limit state region.

When using a GA for mapping the response surface, it is important to obtain an optimal balance between exploration and exploitation [23]. The focus, in this case, should mainly be on exploring the variable space, particularly in the regions of interest, as opposed to when a GA is used as a search routine and the aim is to quickly converge to the optimal point(s). To prevent convergence of the adaptive sampling process to a single point on the limit state surface, a niching technique is used to maintain diversity in the samples around the wider limit state surface. The main steps in the GA adaptive sampling process are described as follows:

Please cite this article in press as: Kingston GB et al. Computational intelligence methods for the efficient reliability analysis of complex flood defence structures. Struct Saf (2010), doi:10.1016/j.strusafe.2010.08.002

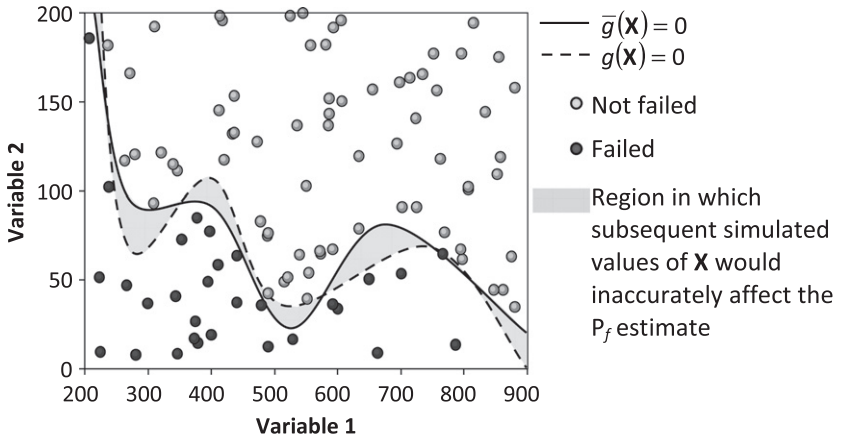

Fig. 4. Potential discrepancy between $g(\mathbf{X})$ and $\bar{g}(\mathbf{X})$ when uniform sampling of the variable space is employed.

Step 1: Define the feasible domain of $\mathbf{X}$ by placing upper and lower limits on the basic variables. Initiate the GA by randomly and uniformly generating an initial population of *chromosomes* (samples) within the defined feasible search space, where each chromosome is made up of a number of *genes* that contain real values of variables.

Step 2: Assess the *fitness* of each individual chromosome by evaluating the corresponding value of the implicit LSF. In this study, the implicit LSF is defined in terms of a factor of safety, F_s, as follows:

$$g(\mathbf{X}) = F_s - 1 \tag{3}$$

where $F_s = R/S$ and failure occurs when $F_s \leqslant 1$. Therefore, the fitness function used to assign the greatest fitness to chromosomes near the limit state surface is given by:

$$\text{Fitness}_i = -(1 - F_{si})^2 \tag{4}$$

where i represents the ith chromosome. The niching technique, known as fitness sharing [24], is then applied to prevent the GA from converging to a single point on the limit state surface. The fitness sharing mechanism is given as follows:

$$\phi(d_{ij}) = \begin{cases} 1 - \left(\frac{d_{ij}}{\sigma}\right) & \text{if } d_{ij} < \sigma \\ 0 & \text{otherwise} \end{cases} \tag{5}$$

where d_{ij} is the distance between samples i and j and σ is the niche radius, or sharing threshold. The parameter $\phi(d_{ij})$ is used to modify the fitness of sample i as follows:

$$\widehat{\text{Fitness}}_i = \frac{\text{Fitness}_i}{\sum_{j=1}^{M} \phi(d_{ij})} \tag{6}$$

where M is the number of samples located within the neighbourhood of the ith individual. In the case where an individual is alone in its niche, its original fitness value remains intact.

Step 3: Select a number of *parent* chromosomes from the population to fill the *mating pool* which contributes offspring to the next generation. In this study, tournament selection [24] was applied, whereby pairs of chromosomes compete to be selected and fitter chromosomes are given a greater chance of contributing to the next generation, whilst less fit chromosomes die out.

Step 4: Apply a genetic crossover operator between pairs of selected parents to produce offspring, which form the next generation of chromosomes. There are a number of different forms of crossover operator. In this paper, the two child staggered average crossover operator [25] was applied, as this operator has been designed to exploit the continuous nature of the variables.

Step 5: Mutation is the final step in the generation of child chromosomes. This ensures that the evolution does not get trapped in unpromising regions of the search space. The step size mutation operator [25] was used in this study, as it was also designed for continuous variables.

Step 6: Steps 2–5 are repeated until some maximum number of generations has been reached. See [24,25] for further details of GAs and their operators.

The primary advantage of the GA adaptive sampling approach is its ability to provide focused samples in the important limit state region; thus, reducing the computational burden involved in training the ANN-based RSF. However, other notable advantages of this method include the following:

- The GA adaptive sampling approach is relatively independent of the dimension of the problem, in that a greater number of samples is not necessarily required for higher dimensional problems.
- Apart from the requirement of upper and lower bounds on the basic variables, the sampling method does not impose any strong assumptions on the model (which includes the basic variables and the actual and approximate LSFs). This gives the method an advantage over, for example, importance sampling methods that require the selection of an appropriate sampling distribution based on assumptions about the problem at hand.
- GA adaptive sampling can handle any shape of the limit state boundary $g(\mathbf{X}) = 0$. As a result, it does not suffer from many of the problems associated with importance sampling methods, such as low sampling efficiency when the limit state function is concave with respect to $\mathbf{X}$, or a non-identifiable unique maximum likelihood point when the limit state function coincides with a contour of $f_{\mathbf{X}}(\mathbf{x})$ the region of interest [4].
- Sampling is performed in real parameter space and therefore no transformations to standard normal space are required.
- The search for the limit state does not require information about the gradient of the LSF and, therefore, does not require that the derivatives of the LSF with respect to the basic variables be estimated.
- The sampling procedure can theoretically be used in conjunction with any LSF (implicit or otherwise) and the flexible fitness function can be defined according to the specific outputs of the model used.

Please cite this article in press as: Kingston GB et al. Computational intelligence methods for the efficient reliability analysis of complex flood defence structures. Struct Saf (2010), doi:10.1016/j.strusafe.2010.08.002

4. Case study – flood wall at 17th Street Canal in New Orleans

4.1. Background

The flooding that took place in New Orleans in August 2005 as a consequence of Hurricane Katrina was widely publicised and well documented (see [1,2] for example). Analysis of the flood protection system in the aftermath of the event has shown three primary mechanisms that led to structural failure of different elements of the protection system: overtopping of concrete "I-wall" structures, leading to rear slope erosion and subsequent structural failure; overtopping causing crest erosion and subsequent failure of earth levees; and the lateral sliding of I-walls due to geotechnical failure when hydraulic loading levels remained below the structure crest levels [26,27]. The latter failure mechanism arose along an I-wall section of the 17th Street drainage canal protection system [27]. This failure, the focus of the case study, is of particular interest due to its below design-level nature and the significantly exacerbated consequences that resulted.

Post event geotechnical analysis has shown that a shear failure surface formed along a clay layer beneath the foundation of the levee and I-wall. The surface extended laterally into the floodplain where it exited vertically through the marshland [27]. Evidence of this type of failure was seen by the the lateral displacement of I-wall sections by 10 m into the floodplain and the vertical uplifting of a wooden hut on the levee by 2.5 m. Finite element models have proved a successful tool in modelling failures of this type.

4.2. Finite element model

Since the 17th Street Canal flood wall breach was geotechnical, complex and catastrophic in nature, the finite element analysis program, PLAXIS [28], was used to analyse the behaviour of this wall. The FE model set up used to model the section is shown in Fig. 5. The geometry of the section was taken from [1], where PLAXIS was also used to perform a FE analysis of the wall section; however, in this study, a somewhat simpler FE model with a less refined mesh was used to save on computation time [29,30]. As can be seen in Fig. 5, the section has seven soil layers, which were described in the model by the 10 resistance soil parameters given in Table 1. The Mohr–Columb and Advanced Soft Soil models were used for predicting the behaviour of the soil layers. Where possible, the Mohr–Columb model was applied in preference to more advanced soil models, as its computational run times are considerably less than the more advanced models and it generally gives good results for failure prediction. All soil parameters were treated as uncertain properties and modelled as random variables. These variables were all assumed to be Gaussian and data from the geotechnical analyses conducted by Independent Levee Investigation Team [1] were used to define the parameters of these distributions (mean and coefficient of variation (CV)), which are also given in Table 1.

The behaviour of the flood wall was modelled for a single given water level (loading condition). The breach that occurred in August 2005 did so when the water level was between 7 ft and 8 ft (2.13–2.44 m) above mean sea level (AMSL) [1]. In the study carried out by Rajabalinejad et al. [30], it was found that the failure probability of the wall at a water level of 8 ft AMSL was 43.6%. However, in this study, the reliability of the flood wall was assessed when subject to a water level of 4 ft (1.22 m) AMSL, since, for fragility, it is necessary to cover the whole range of loading conditions and the advantages of the proposed efficient reliability analysis approach can best be demonstrated at low failure probabilities.

4.3. GA sampling

Using the PLAXIS FE model, the factor of safety F_s against sliding can be calculated using two methods: the first is by the ϕ–C reduc-

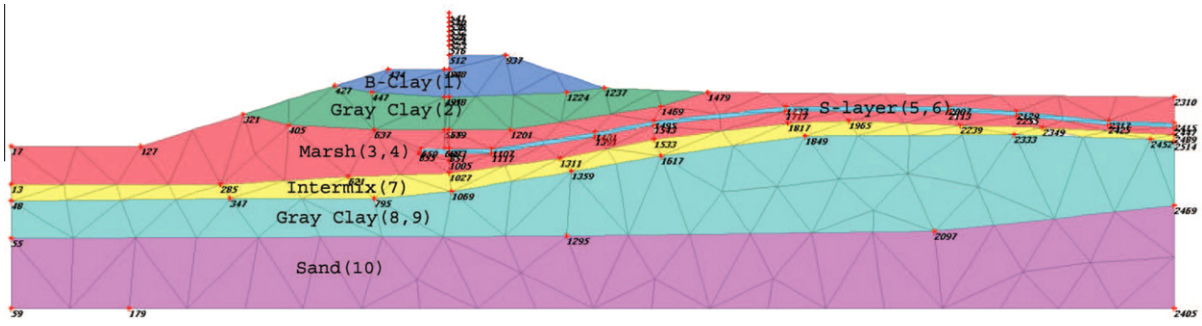

Fig. 5. Plot of the FE model for the 17th street flood wall and its foundation, as modelled with PLAXIS.

Table 1
Soil parameters used in the FE model.

	Soil	Model	Behaviour	Distribution type	Parameter[a]	Mean	CV
1	Brown clay	Mohr–Coulomb	Undrained	Normal	C	900	0.2
2	Gray clay	Mohr–Coulomb	Undrained	Normal	C	600	0.2
3	Marsh under levee	Mohr–Coulomb	Undrained	Normal	C	375	0.3
4	Marsh free field	Mohr–Coulomb	Undrained	Normal	C	200	0.3
5	Sensitive layer – under levee	Mohr–Coulomb	Undrained	Normal	C	200	0.3
6	Sensitive layer – free field	Mohr–Coulomb	Undrained	Normal	C	180	0.3
7	Intermix zone	Soft Soil Model	Undrained	Normal	ϕ	23	0.3
8	Gray clay horizontal	Mohr–Coulomb	Undrained	Normal	C	100	0.3
9	Gray clay vertical	Mohr–Coulomb	Undrained	Normal	C	11	0.3
10	Sand	Mohr–Coulomb	Drained	Normal	ϕ	36	0.3

[a] C-cohesion in pounds per square foot (psf), ϕ- friction angle (deg).

Please cite this article in press as: Kingston GB et al. Computational intelligence methods for the efficient reliability analysis of complex flood defence structures. Struct Saf (2010), doi:10.1016/j.strusafe.2010.08.002

Table 2
Parameter values used in the GA adaptive sampling procedure.

Parameter	Value
Population size	100
No. of generations	20
Probability of crossover	0.7
Probability of mutation	0.2
Mutation step size	0.2
Niche radius	7

tion technique [31], which is only applicable when samples are in the safe domain (i.e. when $g(\mathbf{X}) > 0$) and returns values greater than one. The second method provides a parallel definition of F_s and is applicable only when samples are in the failure domain (i.e. when $g(\mathbf{X}) \leqslant 0$). This method computes the percentage of total loading that will result in structural failure, which returns values less than or equal to one. Whilst these definitions of F_s are similar in their representation, their values are not directly comparable. Therefore, it is more appropriate to use only one method to evaluate (3) on one side of the limit state. The latter method based on percentage of total loading was selected for this, as it is significantly more computationally efficient than the ϕ–C reduction method and it provides a better quality mapping of the response surface in the region of most interest, $g(\mathbf{X}) \leqslant 0$. The fitness function defined by (4) was then used in the sampling process, where F_s was determined by the percentage of total loading when samples lay in the failure domain, whilst samples in the safe domain were assigned a value of $F_s = 2$ (since the percentage of total loading method is not applicable when the structure is in a safe state). Setting $F_s = 2$ for all samples in the safe domain gives these samples an equivalent minimum fitness value to a sample that fails under no loading, which is appropriate given that it is not possible to distinguish between those samples that are close to or far from the limit state $g(\mathbf{X}) = 0$ when the structure does not fail and the percentage of total loading is used to define F_s.

Before beginning the GA sampling process, it was first necessary to define upper and lower limits for the soil parameters given in Table 1. To ensure that the normally distributed soil parameters were not significantly truncated by the limits placed on them and that the resulting sampled parameters could be used to accurately estimate structural reliability, these limits were set equal to 3.5 times the standard deviation on either side of the mean, accounting for greater than 99.9% of possible soil parameter values. It was also necessary to define a number of basic parameters used by the GA. These are given in Table 2. The last four parameters in this table were selected based on values reported in the literature and the characteristics of the problem at hand, whilst the population size and number of generations were selected to allow sufficient convergence to the limit state by the final generations and a sufficient number of overall training samples ($20 \times 100 = 2000$ training samples).

Shown in Fig. 6 are the resulting samples of soil parameter X_3 (marsh under levee) versus soil parameter X_8 (gray clay horizontal) from generations (a) 1–5; (b) 6–10; (c) 11–15; and (d) 16–20 of the GA sampling procedure, where it can be seen that the GA had the desired effect of focusing the sampling toward the limit state surface. In Fig. 6e, which shows all 2000 samples, the success of the procedure in achieving a rather coarse coverage of the entire parameter space with very dense coverage in the important region is demonstrated. The coarse, roughly uniform coverage was achieved primarily in the first 500 samples (Fig. 6a), whilst the last 500 samples (Fig. 6d) are all densely concentrated in a small region of the space. It can also be seen that the number of samples in the failure domain increases dramatically between the first 500 samples and the last. In fact, this proportion increases from 16% (11% in the first generation) to 68% (79% in the 20th generation). It was previously found that soil parameters X_3 and X_8 had the strongest influence on the probability of failure of the 17th Street flood wall [29] and it was, therefore, expected that any patterns of convergence to the limit state would be most evident in these plots. However, it should be noted that similar patterns of convergence were also evident in plots of the other soil parameters.

4.4. ANN-based RSF

The 2000 samples output from the GA sampling process include values of the soil parameters given in Table 1, together with their corresponding values of F_s (where $0 \leqslant F_s \leqslant 1$ in the failure domain and $F_s = 2$ in the safe domain). As these responses do not properly represent the actual implicit LSF in the safe region, it was considered more appropriate to use the ANN model for classification of the failure and safe domains, rather than for functional approximation. Therefore, all values of $F_s \leqslant 1$ were assigned a value of 0 (failure), while responses of $F_s = 2$ were assigned a value of 1 (safe).

The *generalisability* of an ANN, which is its ability to infer a generalised solution to a problem, can be estimated by evaluating its out-of-sample performance on an independent test data set. Therefore, the available 2000 data points were divided into a training set (80%) and a test set (20%) using the SOM data division method described in [32], such that each set maintained similar statistics. A trial and error process was then used to select the appropriate number of hidden layer nodes, whereby a number of networks were trained, while the number of hidden nodes was systematically increased until the network which performed best on the test data was found. Only single hidden layer MLPs with a hyperbolic tangent (tanh) activation function on the hidden layer nodes and logistic sigmoid activation at the output layer were considered in this study, as this configuration is best suited to data classification. The error function used for training was also selected to suit the classification problem and is given by:

$$E = -\sum_{n=1}^{N} [y_n \times \log(\hat{y}_n)] + [(1 - y_n) \times \log(1 - \hat{y}_n)] \tag{7}$$

where y is the actual binary target value of F_s and $\hat{y}$ is the ANN output signal, which, as a result of the logistic sigmoid transfer at the output node, can have values between 0 and 1 (i.e. $\hat{y}$ is the predicted value of binary F_s). There are a number of algorithms available for ANN training, backpropagation being the most popular; however, in this study a GA was also used for training the ANN models developed. This involved a similar approach to that described in Section 3, but it did not involve niching (as the aim was to converge to a single optimal weight vector); fitness was defined as Fitness = $-E$, where E is the error function given by (7); and only the single, optimal weight vector was retained.

Model performance (as opposed to the fitness function used during training) was defined in terms of percentage of samples correctly classified as being in the failure or safe regions. Based on this measure, the results of the trial and error hidden node selection process are shown in Fig. 7. It can be seen that, whilst the percentage of samples correctly classified increases with network size for the training data set, the generalisability does not improve significantly beyond that of the 1-hidden node model. A 2-hidden node ANN was able to classify two additional test cases correctly (resulting in an increase from 95.5% of cases correctly classified to 96%), but the addition of one hidden node results in an ANN model with almost double the number of weights (25 in comparison to 13 for the 1-hidden node ANN). Therefore, a 1-hidden node ANN was selected as the RSF. Overall, this model correctly classified 1917 of the 2000 (95.9%) data samples generated using the GA sampling

Please cite this article in press as: Kingston GB et al. Computational intelligence methods for the efficient reliability analysis of complex flood defence structures. Struct Saf (2010), doi:10.1016/j.strusafe.2010.08.002

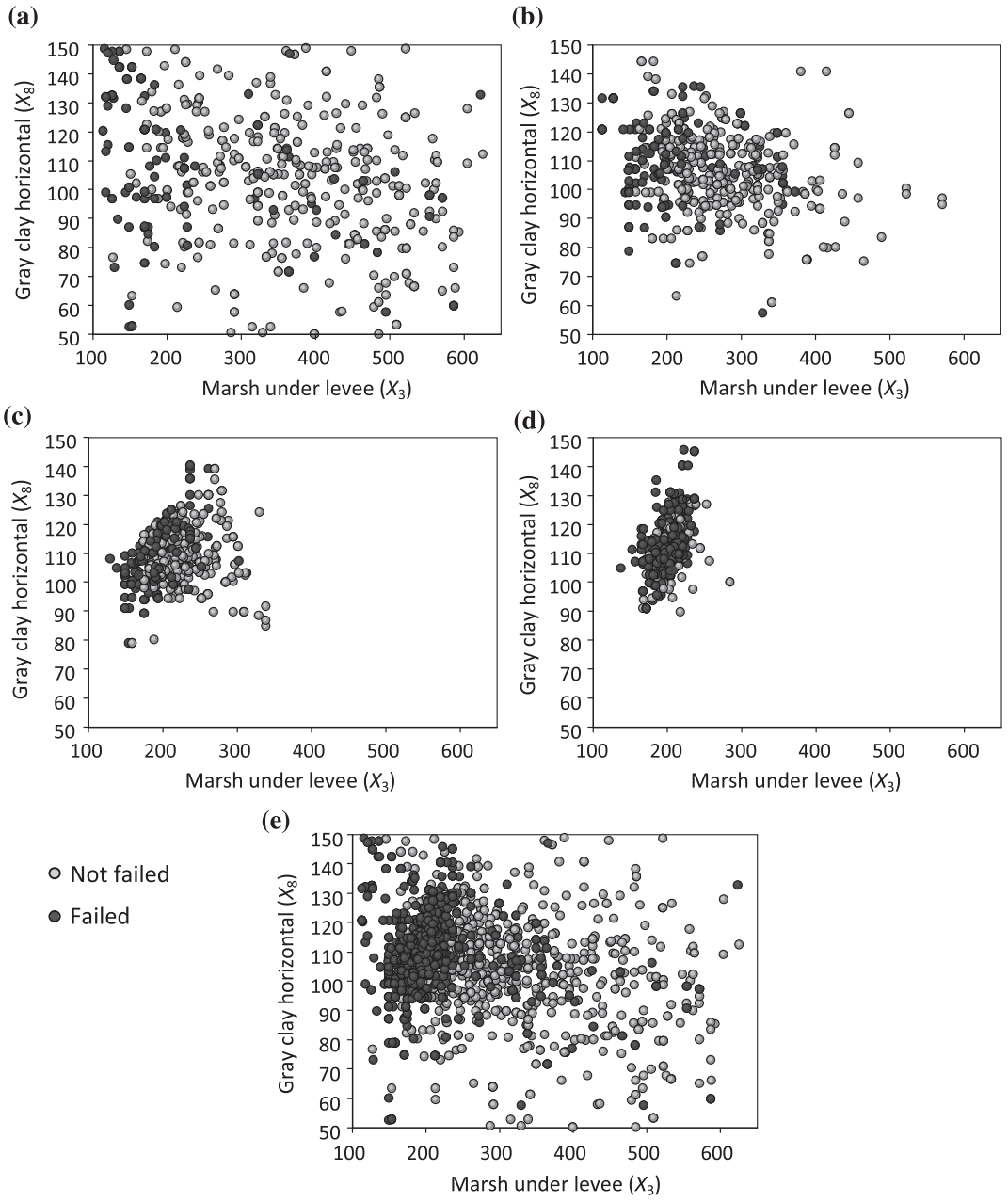

Fig. 6. GA samples from (a) generations 1–5, (b) generations 6–10, (c) generations 11–15, (d) generations 16–20, and (e) all generations.

process, which contained 36.9% defence failed states and 63.1% safe states. Therefore, it was concluded that this model was adequate for the needs of performing a reliability analysis. The 1-hidden node ANN model can be written as a one line equation:

$$\hat{y} = \frac{1}{1 + \exp\left\{-\left[\tanh\left(\sum_{i=1}^{10} w_i X_i + w_{11}\right) \cdot w_{12} + w_{13}\right]\right\}} \tag{8}$$

and can easily be incorporated into a MCS procedure.

4.5. Monte Carlo based reliability analysis

To assess the reliability of the 17th Street Canal flood wall given a water level of 4 ft AMSL, MCS of the selected 1-hidden node ANN model was performed, providing 10,000 predictions of failed and safe defence states corresponding to 10,000 random combinations of the uncertain soil parameters. These results were then processed to determine the probability of failure of the flood wall for this loading situation. As mentioned in Section 1, a MCS was also performed where the failed and safe defence states were computed directly using the complex PLAXIS FE model. This was done in order to gain some appreciation of the level of accuracy and efficiency that can be achieved using the proposed ANN-based RSF. Therefore, both methods used the same sample of soil parameter combinations, which enabled the percentage of defence states correctly classified by the ANN to be assessed.

With direct MCS of the actual LSF, it was found that the 'actual' probability of failure of the flood wall was equal to 16% at a water level of 4 ft AMSL. In comparison, MCS of the ANN-based RSF resulted in an estimated probability of failure of 12%. The ANN was able to correctly classify 93% of the 10,000 MC samples as being in the failed or safe regions, which was considered to be a reason-

Please cite this article in press as: Kingston GB et al. Computational intelligence methods for the efficient reliability analysis of complex flood defence structures. Struct Saf (2010), doi:10.1016/j.strusafe.2010.08.002

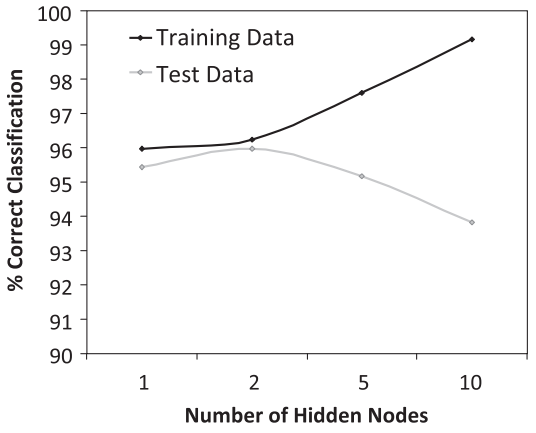

Fig. 7. Number of hidden nodes versus % correct classification rates for the training and test data sets.

able level of accuracy to be achieved by a significantly simpler model. However, of the 7% of samples that were misclassified by the ANN, 78% were in the failure region (as identified by the PLAXIS model), which resulted in the lower than 'actual' estimated failure probability. In the attempt to diagnose why these samples may have been incorrectly classified, all 10,000 samples were clustered into groups of similar input combinations using a Self-Organising Map (SOM) [33]. This has the effect of reducing the multi-dimensional input data to a two-dimensional space, such that any patterns existing within the data are enhanced. If misclassified samples were found to cluster together, this would suggest that significant relationships exist between the soil parameters and the state of the flood wall that were not captured by the ANN.

Shown in Fig. 8 is the 9×10 SOM grid used to cluster the data samples, which was selected based on the resulting within- and between-cluster similarities and dissimilarities, respectively. In this figure, different sized circles are used to represent the different proportions of similar input samples contained in each grid cell that were correctly and incorrectly classified by the ANN model. For example, in cell [9,10], the single dark gray circle indicates that 100% of samples in that cluster were correctly classified by the ANN model, whilst in cell [2,1], the light and dark gray circles of approximately the same size indicate that approximately half of the similar samples in this cell were misclassified. As can be seen, there are no obvious patterns between the clustered input data and the classification results (i.e. misclassified samples do not appear to cluster together), which suggests that no significant input–output relationships remain uncaptured by the ANN. Therefore, it was concluded that possible reasons for misclassification are due to the inner intricacies of the FE model and the inability of these to be represented by the much simpler ANN model, rather than any gross misrepresentations by the ANN model. Where the uncertainties introduced by this approximation are significant, similar approaches to those employed with the traditional RSM can be employed, whereby the differences between the emulator (ANN in this case) and the actual response surface are represented through an error term [4].

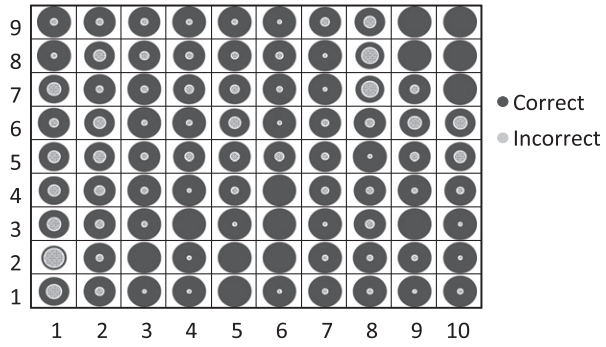

Fig. 8. SOM grid displaying clustered data samples.

The total time required to develop and run the ANN-based RSF within a MCS is dependent upon the time required to generate the training and test data using the GA adaptive sampling method; the time taken to train a number of ANN models in order to select the appropriate complexity; and the time required to run the ANN for the required number of MC samples. For complex LSFs, the majority of time is spent on the first component; generating the data. Therefore, the efficiency of the proposed ANN-based approach can be assessed based primarily on the average time required for one evaluation of the implicit LSF and the number of evaluations required to develop an ANN-based RSF, in comparison to the number of evaluations required for direct MCS with the PLAXIS model. In this study, the time required for one evaluation of the PLAXIS FE model was approximately 1 min. Therefore, the computational time required for the direct MCS was approximately 1 week, in comparison to the 1.4 days required by the ANN-based RSF method (and the 1.6 h required to train and select from four different ANN models and the 5 s taken to perform a MCS of the 1-hidden node ANN-based RSF). Whilst this may not seem like a sufficiently significant saving in computation time to warrant the application of the proposed technique, flood defence reliability is typically represented by fragility curves, which give the probability of failure conditional on a range of loading conditions (see 2). To develop a fragility curve for the 17th Street Canal flood wall given a range of water levels between 4 ft and 9 ft with a 1 ft increment (i.e. six loading conditions) would take approximately 6 weeks using direct MCS of the PLAXIS model, whilst it would take just over 1 week (8.4 days) using the ANN-based RSF approach. Therefore, the savings in computation time gained through the increased efficiency of the proposed ANN-based RSF method become much more beneficial, with the actual savings achieved being proportional to the complexity of the FE model.

5. Conclusions

In this paper, an ANN-based RSF approach for producing robust estimates of complex failure probabilities given limited evaluations of the actual implicit LSF has been presented. The method can, in principle, be applied to situations and is most appropriate for application when evaluation of the LSF is computationally demanding. The GA adaptive sampling procedure used to generate the training samples overcomes the limitations of standard MCS or uniform sampling strategies in problems with low failure probability by focusing the sampling toward the important limit state region and, as a result, enabling a more accurate representation of the actual implicit LSF in the region in which it most impacts the failure probability estimate. The focus of the proposed approach was not on achieving maximum gains in computational efficiency, but rather on developing a robust method for flood defence reliability analysis that takes advantage of both the improvements in efficiency that can gained through using a simplified model to emulate a complex response surface and through the continual improvements to computer hardware. Therefore, the approach is seemingly less (algorithmically) efficient than the original RSM, which, by necessity, relied upon very few calls to the actual LSF, but involved some rather crude approximations to the problem (e.g. the quadratic RSFs which provided insufficient representation of the actual LSF). However, in the development of new structural reliability analysis procedures, the improvements to efficiency that

Please cite this article in press as: Kingston GB et al. Computational intelligence methods for the efficient reliability analysis of complex flood defence structures. Struct Saf (2010), doi:10.1016/j.strusafe.2010.08.002

are continually being gained through improvements to computer hardware should not be ignored, as such improvements generally mean that less approximate and more robust methods can be developed.

The ANN-based RSF method, combined with GA adaptive sampling, is most beneficial for assessing the reliability of critical flood defences where failure could result in catastrophic flooding and for which there are sufficient geotechnical data to define variations in the soil foundation. Such methods are expected to become increasingly important in future, as sea levels rise and existing flood defences age and deteriorate, no longer providing the targeted standard of protection they were designed to achieve. The 2005 New Orleans flood event, where the catastrophic failure of flood defences occurred when water levels were below design elevations, highlighted the fact that it is no longer appropriate to offer a single assured standard of protection from flooding, but rather that it is necessary to assess the reliability of flood defence systems over time under varying conditions. The proposed method offers an efficient means for analysing critical defence reliabilities, where actual structural properties are considered instead of those assumed for design purposes, which will aid in the identification of system vulnerabilities and the minimisation or avoidance of future catastrophes related to critical flood defence failures.

Appendix A. Feedforward multilayer perceptron

There are many different types of ANNs in terms of structure and mode of operation. These are generally classified according to network topology and type of connectivity between the nodes, the type of data used, the way in which the network 'learns' the underlying function and the computations performed by each node. Feedforward multilayer perceptrons (MLPs) are a very popular and widely used ANN structure for prediction and response surface approximation problems.

The general structure of a MLP is illustrated in Fig. 9. The input layer receives input information, generally in the form of a vector of observed or pre-processed data values $\mathbf{x} = \{x_i, i = 1,\ldots,K\}$, where K is the number of input or predictor variables. No processing occurs at this layer, rather the input layer nodes serve only to transmit the input information, in a feedforward direction, to subsequent layers in the network. This is done via weighted connections, where each node in the input layer is connected to every node in the first hidden layer, such that the input information is redistributed across the all of the nodes in the hidden layer. The input to the jth node in the first hidden layer is then the sum of the weighted values from the input layer with the addition of a weighted offset, or *bias*, term:

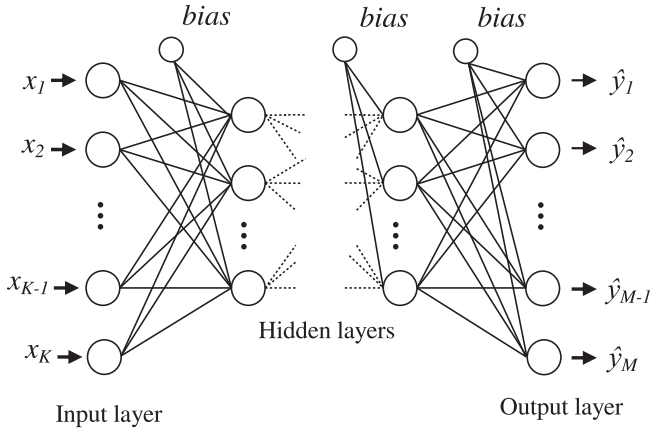

Fig. 9. General structure of a MLP.

$$zin_j = w_{0j}x_0 + \sum_{i=1}^{k} w_{ij}x_i \tag{9}$$

where x_0 denotes the bias and is typically set equal to 1. The result zin_j is then transformed by the node's transfer, or activation, function to generate an activation level for that node (see Fig. 3):

$$z_j = h(zin_j) \tag{10}$$

The transfer function $h()$ may be any continuous differentiable function, but is commonly sigmoidal at the hidden layer nodes or linear at the output layer. Each of the activations from the first hidden layer nodes are then transmitted to and processed by the nodes in the subsequent layer in a similar fashion to that described for the first hidden layer. This process is continued until the information reaches the output layer. The activation level generated at the mth output node is the prediction $\hat{y}_m$ of the mth dependent variable of interest.

The "training" of a MLP can be compared to the calibration of coefficients in statistical models. During training the aim is to find values for the connection and bias weights so that the outputs produced by the ANN approximate the observed training data well. ANNs, like all mathematical models, work on the assumption that there is a real function underlying a system that relates a set of K independent predictor variables $\mathbf{x}^K$ to M dependent variables of interest $\mathbf{y}^M$. Therefore, the overall aim of ANN training is to infer an acceptable approximation of this relationship from the training data, so that the model can be used to produce accurate predictions when presented with new data. Thus, if the function relating the measured target data to the model inputs is given by:

$$\mathbf{y}^M = f(\mathbf{x}^k, \mathbf{w}) \tag{11}$$

where $f(\cdot)$ is the function described by the MLP, $\mathbf{w}$ is a vector of weights that characterise the data generating relationship, the aim is to find the best estimate of the weight vector. This is typically done by iteratively adjusting and optimising the weights such that some function of the difference between the measured target data $\mathbf{y}^M$ and the predicted outputs $\hat{\mathbf{y}}^M$ (e.g. the sum squared error $E_{\mathbf{y}} = \frac{1}{2}\sum(\mathbf{y}^M - \hat{\mathbf{y}}^M)^2$) is minimised.

References

[1] Independent Levee Investigation Team. Investigation of the performance of the New Orleans flood protection systems in Hurricane Katrina on August 29, 2005, Final report; 2006. <http://walrus.wr.usgs.gov/geotech/katrina/images/Katrina_Final_VOL_1.pdf>.
[2] Interagency Performance Evaluation Task Force (IPET). Performance evaluation of the New Orleans and Southeast Louisiana hurricane protection system. Executive summary and overview, vol. I. Final report, US Army Corps of Engineers; 2008.
[3] The Pitt Review. Learning Lessons from the 2007 Floods, Final report. Cabinet Office, London (UK); 2008.
[4] Melchers RE. Structural reliability analysis and prediction. 2nd ed. New York: Wiley; 1999.
[5] Gouldby B, Sayers P, Mulet-Marti J, Hassan MAAM, Benwell D. A methodology for regional-scale flood risk assessment. Water Manage – Proc Inst Civil Eng 2008;161(3):169–82.
[6] Bucher CG, Bourgund U. A fast and efficient response surface approach for structural reliability problems. Struct Safety 1990;7(1):57–66.
[7] Rajashekhar MR, Ellingwood BR. A new look at the response surface approach for reliability analysis. Struct Safety 1993;12(3):205–20.
[8] Schueller GI, Bucher CG, Bourgund U, Ouypornprasert W. On efficient computational schemes to calculate structural failure probabilities. Probabilist Eng Mech 1989;4(1):10–8.
[9] Kim S-H, Na S-W. Response surface method using vector projected sampling points. Struct Safety 1997;19(1):3–19.
[10] Hurtado JE. An examination of methods for approximating implicit limit state functions from the viewpoint of statistical learning theory. Struct Safety 2004;26(3):271–93.
[11] Hurtado JE, Alvarez DA. Neural-network-based reliability analysis: a comparative study. Comput Methods Appl Mech Eng 2001;191(1–2):113–32.
[12] Cabral SVS, Katafygiotis L. Neural network based response surface method and adaptive importance sampling for reliability analysis of large structural systems. In: Corotis RB, Schueller GI, Shinozuka M, editos. Structural safety

and reliability, proceedings of the 8th international conference of structural safety and reliability, ICOSSAR'01, vol. 2. Newport Beach (CA): Balkema Publishers; 2001 [CD-ROM].
[13] Hurtado JE. Analysis of one-dimensional stochastic finite elements using neural networks. Probabilist Eng Mech 2002;17(1):35–44.
[14] Papadrakakis M, Papadopoulos V, Lagaros ND. Structural reliability analysis of elastic–plastic structures using neural networks and Monte Carlo simulation. Comput Methods Appl Mech Eng 1996;136(1–2):145–63.
[15] Papadrakakis M, Lagaros ND. Reliability-based structural optimization using neural networks and Monte Carlo simulation. Comput Methods Appl Mech Eng 2002;191(32):3491–507.
[16] Papadrakakis M, Papadopoulos V, Lagaros ND, Oliver J, Hue-spe AE, Sanchez P. Vulnerability analysis of large concrete dams using the continuum strong discontinuity approach and neural networks. Struct Safety 2008;30(3): 217–35.
[17] Cheng J, Li QS, Xiao R-C. A new artificial neural network-based response surface method for structural reliability analysis. Probabilist Eng Mech 2008;23(1):51–63.
[18] Most T, Bucher C. Probabilistic analysis of concrete cracking using neural networks and random fields. Probabilist Eng Mech 2007;22(2):219–29.
[19] Cheng B, Titterington DM. Neural networks: a review from a statistical perspective. Stat Sci 1994;9(1):2–30.
[20] Bishop CM. Neural networks for pattern recognition. Oxford: Oxford University Press; 1995.
[21] McCulloch WS, Pitts W. A logical calculus of ideas immanent in nervous activity. Bull Math Biophys 1943;5:115–33.
[22] Cheng J, Li QS. Reliability analysis of structures using artificial neural network based genetic algorithms. Comput Methods Appl Mech Eng 2008;197(45–48): 3742–50.
[23] Khu ST, Werner MGF. Reduction of Monte-Carlo simulation runs for uncertainty estimation in hydrological modelling. Hydrol Earth Syst Sci 2003;7(5):680–92.
[24] Goldberg DE. Genetic algorithms in search, optimization and machine learning. Reading (Mass.): Addison-Wesley Pub. Co.; 1989.
[25] Vitkovsky JP, Simpson AR, Lambert MF. Leak detection and calibration using transients and genetic algorithms. J Water Resour Plann Manage 2000;126(4):262–5.
[26] Nicholson P, Francisco S-T. Reconnaissance of levee failures after hurricane Katrina. Proc Inst Civil Eng – Civil Eng 2008;161(3):124–31.
[27] Interagency Performance Evaluation Task Force (IPET). Performance evaluation of the New Orleans and Southeast Louisiana hurricane protection system. The performance – levees and floodwalls, vol. V. Final report. US Army Corps of Engineers; 2007.
[28] PLAXIS BV. PLAXIS finite element code for soil and rock analyses; 2006. <www.plaxis.nl>.
[29] Rajabalinejad M, Kanning W, Van Gelder PHAJM, Vrijling JK, Van Baars S. Probabilistic assessment of the flood wall at 17th Street canal, New Orleans. In: Aven T, Vinnem JE, editors. Proceedings of the European safety and reliability conference (ESREL 2007). Taylor and Francis Group, Stavanger, Norway; 2007.
[30] Rajabalinejad M, Van Gelder PHAJM, Vrijling JK. Probabilistic finite elements with dynamic limit bounds; a case study: 17th Street flood wall, New Orleans. In: Proceedings of the 6th international conference on case histories in geotechnical engineering, Arlington, Virginia; 2008.
[31] PLAXIS BV, PLAXIS 2D 8.0, 3: reference manual; 2006.
[32] Bowden G, Maier H, Dandy G. Optimal division of data for neural net-work models in water resources applications. Water Resour Res 2002;38(2):1010.
[33] Kohonen T. Self-organised formation of topologically correct feature maps. Biol Cybernet 1982;43:59–69.

Please cite this article in press as: Kingston GB et al. Computational intelligence methods for the efficient reliability analysis of complex flood defence structures. Struct Saf (2010), doi:10.1016/j.strusafe.2010.08.002